58th ARFTG Conference Digest, **pp. 35-48, San Diego, CA, Nov. 2001.**

A Method of Developing Frequency-Domain Models for Nonlinear Circuits Based on Large-Signal Measurements*

Jeffrey Jargon[1], K.C. Gupta[2], Dominique Schreurs[3], Kate Remley[1], and Donald DeGroot[1]
[1]National Institute of Standards and Technology
325 Broadway, M/S 813.01, Boulder, CO 80305, USA
Tel: 303.497.3596 | Fax: 303.497.3970 | E-mail: jargon@boulder.nist.gov
[2]University of Colorado at Boulder, Boulder, CO 80309, USA
[3]Katholieke Universiteit Leuven, B-3001 Heverlee, BELGIUM

Abstract **- We describe a method of generating models for nonlinear devices and circuits, based upon measurements of travelling-wave voltages at a periodic large-signal excitation and its harmonics using a nonlinear vector network analyzer. Utilizing a second source, we use multiple measurements of a nonlinear circuit to train artificial neural network models that yield portable, nonlinear large-signal scattering parameters. We obtain an independent check by comparing an example diode-circuit model generated by means of this methodology with a harmonic-balance simulation.**

I. INTRODUCTION

Vector network analyzers (VNAs) are one of the most versatile instruments in the RF and microwave industry. They measure complex scattering parameters (*S*-parameters) of devices or circuits. Engineers use them to verify their designs, confirm proper performance, and diagnose failures. A VNA works by exciting a linear device under test (DUT) with a series of sine-wave signals, one frequency at a time, and detecting the response of the DUT at its signal ports. Since the DUT is linear, the input and output signals have the same frequency as the source, and can be described by complex numbers that account for the signals' amplitudes and phases. The input-output relationships are described by ratios of complex numbers known as *S*-parameters. For a two-port network, four *S*-parameters completely describe the behavior of a linear DUT when excited by a sine wave at a particular frequency.

Although the measurement of *S*-parameters by VNAs is invaluable to the microwave designer for modeling and measuring linear circuits, this is oftentimes inadequate for nonlinear circuits since nonlinearities transfer energy from the stimulus frequency to products at new frequencies. Thus, a different, more sophisticated instrument is required to measure nonlinear devices and circuits. A recently introduced nonlinear vector network analyzer (NVNA) is capable of providing accurate waveform vectors by acquiring and correcting the magnitude and phase relationships between the fundamental and harmonic components in the periodic signals [1-5]. An NVNA excites a nonlinear DUT with one or more sine-wave signals and detects the response of the DUT at its signal ports. Assuming the DUT exhibits neither sub-harmonic nor chaotic behavior, the input and output signals will be combinations of sine-wave signals, due to

the nonlinearity of the DUT in conjunction with mismatches between the system and the DUT. If a single excitation frequency is present, new frequency components will appear at harmonics of the excitation frequency, and if multiple excitation frequencies are present, new frequencies components will appear at the intermodulation products as well as at harmonics of each of the excitation frequencies.

With these facts in mind, the major difference between a linear VNA and an NVNA is that a VNA measures ratios between input and output waves one frequency at a time, while an NVNA measures the actual input and output waves simultaneously over a broad range of frequencies.

So even though *S*-parameters are oftentimes inadequate for representing nonlinear circuits, some type of parameters relating incident and reflected signals are beneficial for modeling purposes. In this paper, we propose definitions of such parameters that we refer to as nonlinear large-signal *S*-parameters.

Unlike linear *S*-parameters, which can be directly calculated from vector network analyzer measurements, nonlinear large-signal *S*-parameters cannot be directly determined from available instrumentation. An NVNA can accurately measure the amplitude and phase of a limited number of spectral components of both the complex incident (a_{ik}) and reflected (b_{ik}) travelling voltage waves, where the subscripts i and k denote the port number and spectral component number, respectively. These travelling-wave voltages, however, cannot be simply ratioed to form nonlinear large-signal *S*-parameters.

In the following sections, we define nonlinear large-signal *S*-parameters, and describe a method for generating them by training artificial neural networks (ANNs) with a number of measurements made on an NVNA using a second source. We then compare a diode circuit model we generate using this method with a harmonic balance simulation. We conclude with a discussion of how these nonlinear large-signal *S*-parameters can be applied to the design of nonlinear devices and circuits.

A similar approach has been used in reference [6] where ‘nonlinear scattering functions’ were introduced by linearizing the nonlinear behavior around an operating point of a bipolar transistor used in a power amplifier. The formulation presented here does not involve any linearization and thus has potentially wider applicability.

II. NONLINEAR LARGE-SIGNAL S-PARAMETERS

Like commonly used linear *S*-parameters, nonlinear large-signal *S*-parameters can also be defined as ratios of incident and reflected wave variables. However, unlike linear *S*-parameters, nonlinear large-signal *S*-parameters depend upon the signal magnitude and must take into account the harmonic content of the input and output signals since energy can be transferred to other frequencies in a nonlinear device. For simplicity, we first consider a two-port network, although this approach can be generalized to any number of ports.

For a two-port network, we have four *S*-parameters for a given power level, bias condition, spectral component number *k* (where *k* is a positive integer), and a specified reference impedance. When a device under test (DUT) is excited at port 1 by a single-tone signal (a_{11}) at a frequency f_1, we define an input reflection coefficient as

$$S_{11k} = \frac{b_{1k}}{a_{11}} \left| \begin{array}{l} a_{2k} = 0 \text{ for all } k \\ a_{1k} = 0 \text{ for } k \neq 1 \end{array} \right. , \quad \textbf{(1)}$$

where a_{jk} and b_{ik} refer to the complex incident and reflected travelling voltage waves, respectively, S_{ijk} indicates the nonlinear large-signal *S*-parameter, the subscripts *i* and *j* denote the port numbers, and *k* is the spectral component number. The forward transmission coefficient is defined as

$$S_{21k} = \frac{b_{2k}}{a_{11}} \left| \begin{array}{l} a_{2k} = 0 \text{ for all } k \\ a_{1k} = 0 \text{ for } k \neq 1 \end{array} \right. . \quad \textbf{(2)}$$

Likewise, when a DUT is excited at port 2 by a signal (a_{21}) at a frequency f_1, we define a reverse transmission coefficient as

$$S_{12k} = \frac{b_{1k}}{a_{21}} \left| \begin{array}{l} a_{1k} = 0 \text{ for all } k \\ a_{2k} = 0 \text{ for } k \neq 1 \end{array} \right. , \quad \textbf{(3)}$$

and an output reflection coefficient as

$$S_{22k} = \frac{b_{2k}}{a_{21}} \left| \begin{array}{l} a_{1k} = 0 \text{ for all } k \\ a_{2k} = 0 \text{ for } k \neq 1 \end{array} \right. . \quad \textbf{(4)}$$

These nonlinear large-signal *S*-parameters S_{ijk} are functions of the excitation levels, in addition to being dependent on bias levels and on the frequency of operation.

This definition of nonlinear large-signal *S*-parameters may be generalized to *N*-port networks as:

$$S_{ijk} = \frac{b_{ik}}{a_{j1}} \left| \begin{array}{l} a_{lk} = 0 \text{ for all } k \text{ \& all } l, l \neq j \\ a_{jk} = 0 \text{ for } k \neq 1 \end{array} \right. , \quad \textbf{(5)}$$

where *j* and *i* respectively refer to the port numbers corresponding to the *a* and *b* travelling waves of interest.

III. METHODOLOGY

The nonlinear large-signal *S*-parameters defined above cannot be determined directly from measurements on a currently available nonlinear network analyzer since impedance mismatches and harmonics from the source cannot be eliminated in these instruments. The nonlinear DUT, in conjunction with the impedance mismatches and harmonics from the source make it impossible to set all of the *a*'s other than a_{11} (assuming port 1 excitation) to zero. In order to overcome this obstacle, we propose a method that makes use of multiple measurements of the DUT using a second source and couplers, as shown in Figure 1. This measurement set-up is identical to that introduced by Verspecht et al. [6] to generate 'nonlinear scattering functions.'

To illustrate our technique, let us first consider the case when a DUT is excited at port 1 by a single-tone signal at frequency f_1 and power level $|a_{11}|$. Utilizing a second source, multiple measurements of a nonlinear circuit are taken for different values of a_{1k} ($k\neq1$) and a_{2k} (for all k), where k is once again the spectral component. These data are then used to develop an ANN model that maps values of *a*'s to *b*'s, as shown in Figure 2.

The nonlinear large-signal *S*-parameters are obtained from the ANN model by interpolating *b*'s from measured results for nonzero values of a_{1k} ($k\neq1$) and a_{2k} (for all k) to the desired values for a_{1k} ($k\neq1$) and a_{2k} (for all k) equal to zero, as shown in Figure 3. Outputs of the ANN model shown in this figure yield values of nonlinear large-signal *S*-parameters S_{11k}.

A similar procedure can be used when a DUT is excited at port 2 by a single-tone signal (a_{21}) at a frequency f_1. In this case, multiple measurements of a nonlinear circuit are made for different values of a_{2k} ($k\neq1$) and a_{1k} (for all k). These data are used to develop an ANN model that maps values of *a*'s to *b*'s (and hence yields nonlinear large-signal *S*-parameters) for a_{2k} ($k\neq1$) and a_{1k} (for all k) equal to zero. Here, the ANN models are used to interpolate *b*'s from measured results for nonzero values of a_{2k} ($k\neq1$) and a_{1k} (for all k) to the desired values for a_{2k} ($k\neq1$) and a_{1k} (for all k) equal to zero. ANN models derived from these measurements will yield values of S_{j2k} (j=1,2).

The ANN architecture used for this modeling is a feedforward, three-layer perceptron structure (MLP3) consisting of an input layer, a hidden layer, and an output layer, as shown in Figure 4. The hidden layer allows complex models of input-output relationships. According to [7], an MLP3 with one hidden signmoidal layer is able to model almost any physical function accurately, provided that a sufficient number of hidden neurons are available. ANNs learn relationships among sets of input-output data, which are characteristic of the device or system under consideration. After the input vectors are presented to the input neurons and the output neurons are computed, the ANN outputs are compared to the desired outputs, and errors are calculated. Error derivatives are then calculated and summed for each weight until all of the training sets have been presented to the network. The error derivatives are used to update the weights for the neurons, and training continues until the errors reach prescribed low levels. In this study, we utilized software developed by Zhang et al. [8] to construct the ANN models.

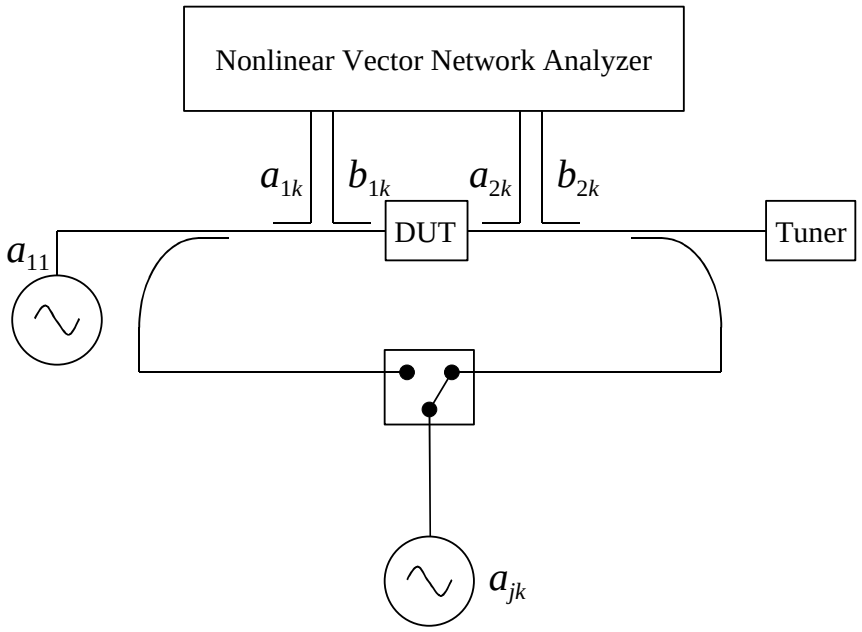

(a)

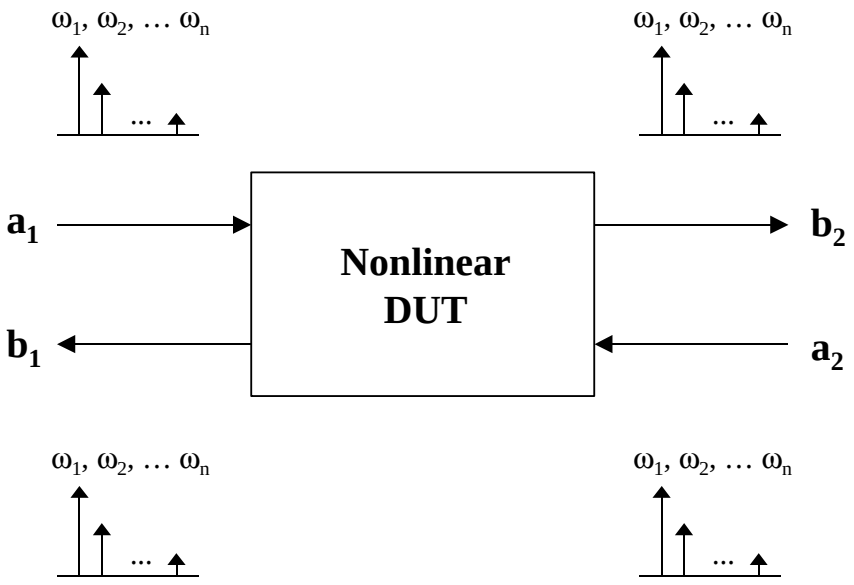

(b)

Figure 1. (a) Block diagram of nonlinear vector network analyzer with a second source. (b) Flow diagram of measurements made with a nonlinear vector network analyzer showing vectors of incident and reflected wave variables.

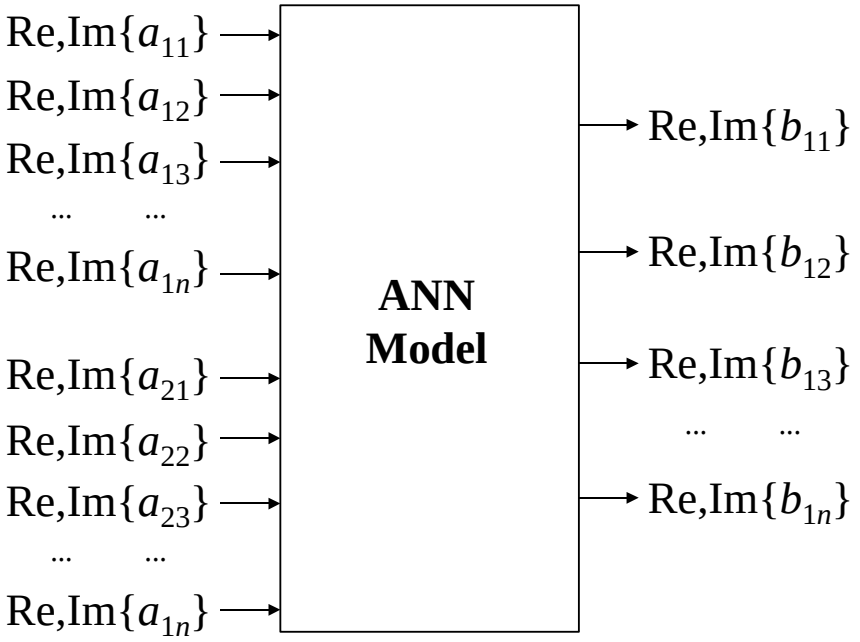

Figure 2. An ANN model that maps real and imaginary values of *a*'s to *b*'s for different real and imaginary values of a_{1k} ($k \neq 1$) and a_{2k} (for all k).

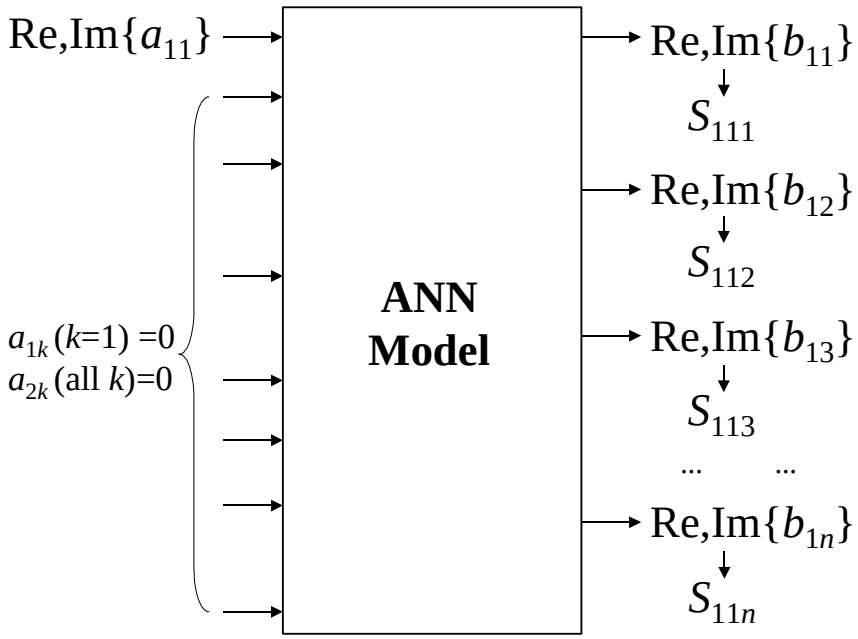

Figure 3. Using an ANN model to interpolate *b*'s from measured results for nonzero values of a_{1k} ($k \neq 1$) and a_{2k} (for all k) to the desired values for a_{1k} ($k \neq 1$) and a_{2k} (for all k) equal to zero. Outputs of the ANN model yield values of S_{11k}.

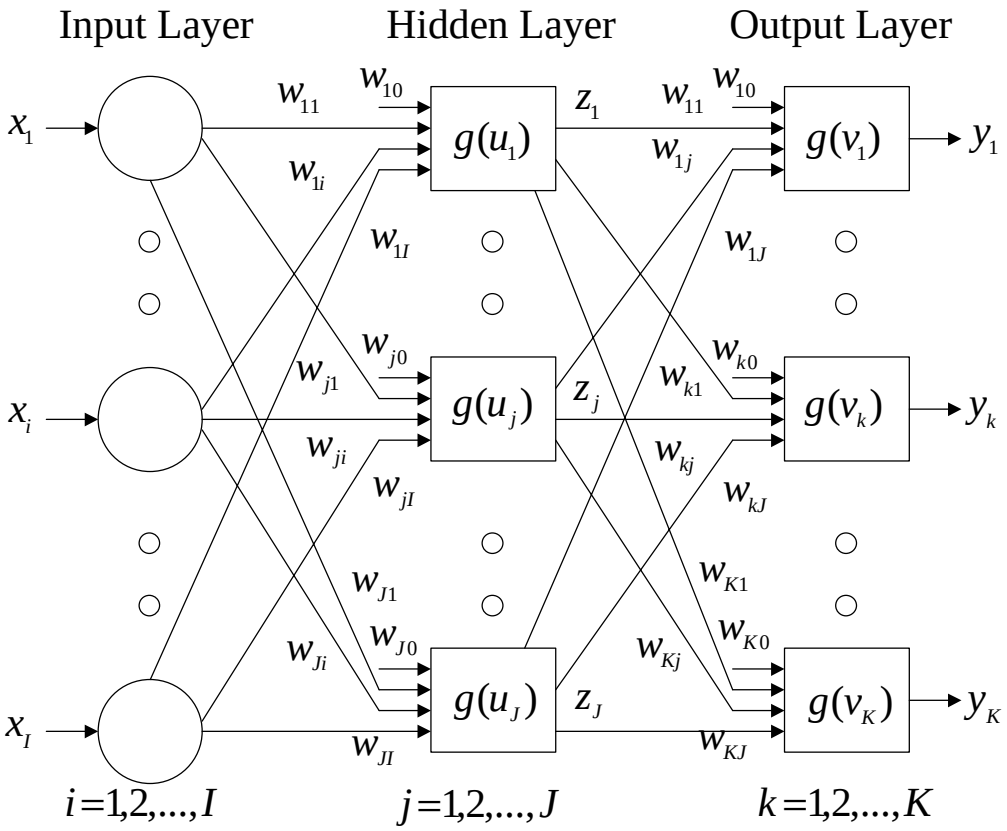

Figure 4. Artificial neural network architecture used for modeling nonlinear large-signal scattering parameters.

IV. MEASUREMENTS AND ANN TRAINING

To test our method of generating nonlinear large-signal *S*-parameters, we developed and fabricated a wafer-level test circuit using a Schottky diode in a series configuration, as shown in Figure 5. The two-port diode circuit was fabricated on an alumina substrate by bonding a beam-lead diode package to the gold metalization layer with silver epoxy. The diode was located in the middle of the coplanar waveguide (CPW) transmission lines, with short lines connecting the diode to probe pads at both ports.

We measured the nonlinear test circuit on an NVNA, an instrument capable of providing accurate waveform vectors by acquiring and correcting the magnitude and phase relationships between the fundamental and harmonic components in the periodic signals [4]. We used an on-wafer line-reflect-reflect-match (LRRM) VNA calibration, along with signal amplitude and phase calibrations [5]. This process places the reference plane at the tips of the wafer probes used to connect with the CPW leads.

For all measurements, the first source, located at port 1, was set to a sine-wave excitation of frequency 1 GHz and magnitude a_{11} = 0.7 V at the probe tips. The second source was connected to port 2 and was set to a sine-wave excitation of frequency 1 GHz and $|a_{21}|$ = 0.7 V at the probe tips. The diode was reversed biased to –0.4 V at port 2, through the probe tips. In order to obtain the nonlinear large-signal *S*-parameters, S_{11k} and S_{21k}, the excitation from source 1 was held constant, while the phase of source 2 was randomly changed for 30 different measurements. Figure 6 plots the resulting measurements of a_{21} in the complex plane. The nonlinearities in the test circuit, along with impedance mismatches, caused signals to be generated at higher harmonics, as shown in Figures 7-10 for the second and third harmonics (a_{12}, a_{13}, a_{22}, and a_{23}). These harmonics varied in magnitude and phase around the origin. This effect allowed nonlinear large-signal *S*-parameters to be obtained from an ANN model, interpolating *b*'s from the measured results for nonzero values of a_{1k} ($k\neq1$) and a_{2k} (for all k) to the desired values for a_{1k} ($k\neq1$) and a_{2k} (for all k) equal to zero.

Data from the 30 measurements were used to develop two ANN models, one for mapping values from the first three harmonics of a (a_{11}, a_{12}, a_{13}, a_{21}, a_{22}, and a_{23}) to b_{11}, and the other for mapping values from the first three harmonics of a to b_{21}. Twenty-six points were used to train each ANN model, and the remaining four points were used as testing data. The testing error was 0.87% for b_{11} and 3.50% for b_{21}, with respective correlation coefficients of 0.99998 and 0.99682. Figures 11 and 12 plot the thirty measurements of b_{11} and b_{21}, respectively.

Once the ANN models were developed, the nonlinear large-signal *S*-parameters, S_{111} and S_{211}, were obtained from eqs. (1) and (2) by interpolating b_{11} and b_{21} from measured results for nonzero values of a_{12}, a_{13}, a_{21}, a_{22}, and a_{23} to the desired values for a_{12}, a_{13}, a_{21}, a_{22}, and a_{23} equal to zero. Figure 11 shows the interpolated value of b_{11} ($=S_{111}\bullet a_{11}$) when a_{12}, a_{13}, a_{21}, a_{22}, and a_{23} are equal to zero, and Figure 12 shows the interpolated value of b_{21} ($=S_{211}\bullet a_{11}$) when a_{12}, a_{13}, a_{21}, a_{22}, and a_{23} are equal to zero.

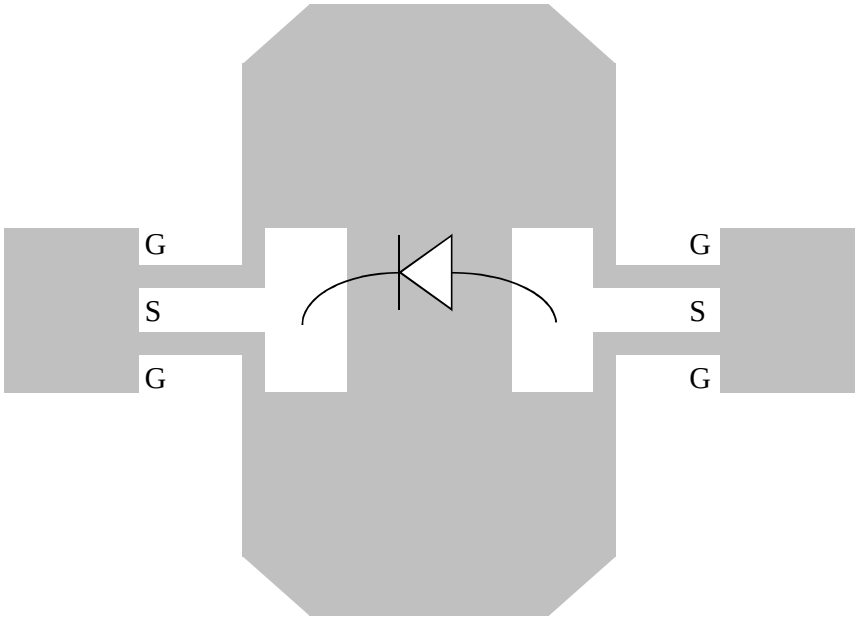

Figure 5. Schottky diode in a series configuration located in the middle of a CPW transmission line. (White area is metal.)

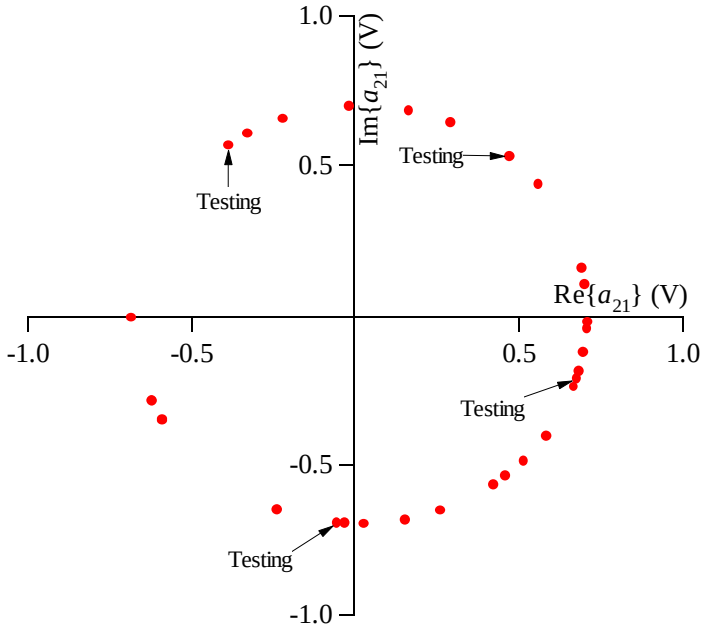

Figure 6. Thirty measurements of a_{21} in the complex plane with the excitation from source 1 held constant and the output from source 2 set to random phases with constant amplitude.

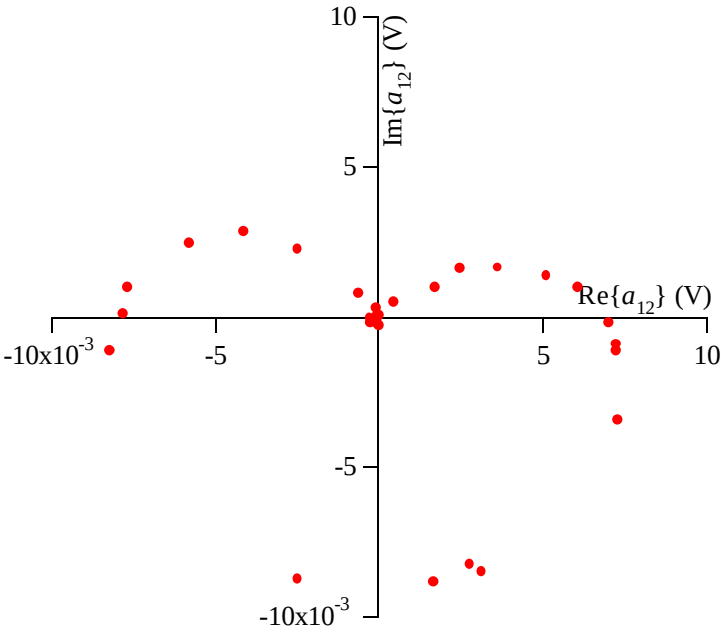

Figure 7. Thirty measurements of a_{12} in the complex plane with the excitation from source 1 held constant and the output from source 2 set to random phases with constant amplitude.

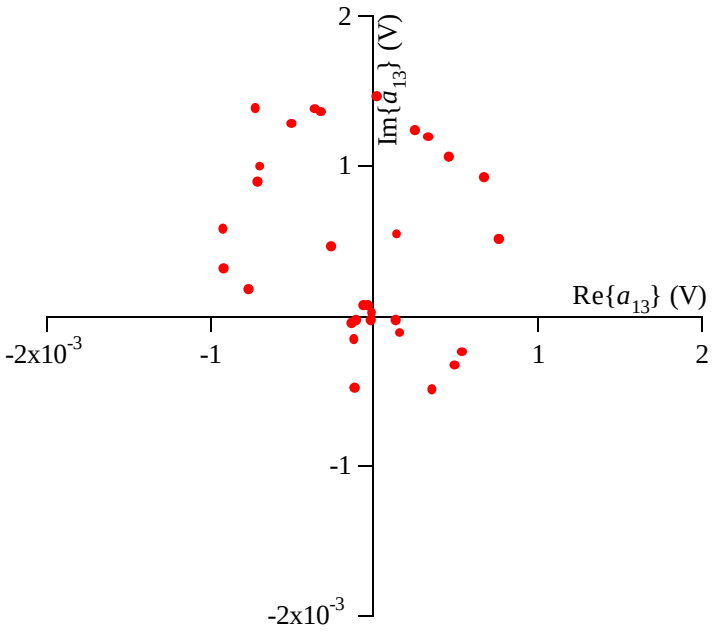

Figure 8. Thirty measurements of a_{13} in the complex plane with the excitation from source 1 held constant and the output from source 2 set to random phases with constant amplitude.

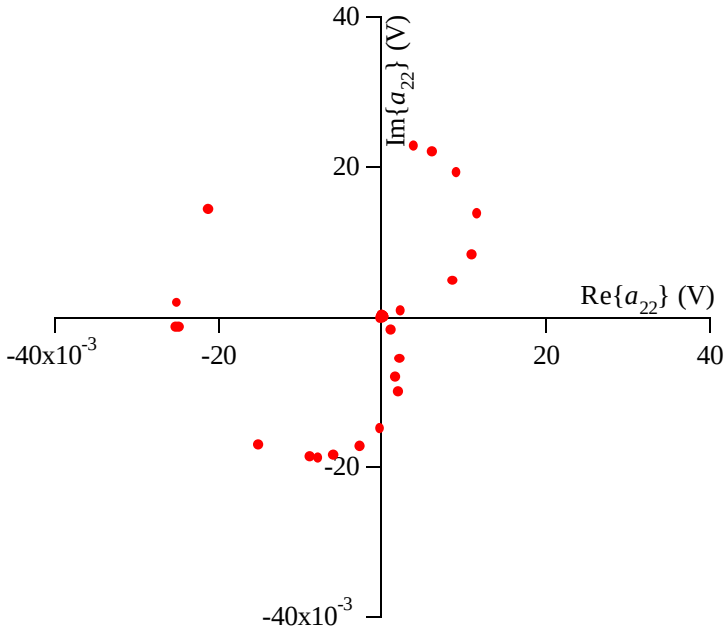

Figure 9. Thirty measurements of a_{22} in the complex plane with the excitation from source 1 held constant and the output from source 2 set to random phases with constant amplitude.

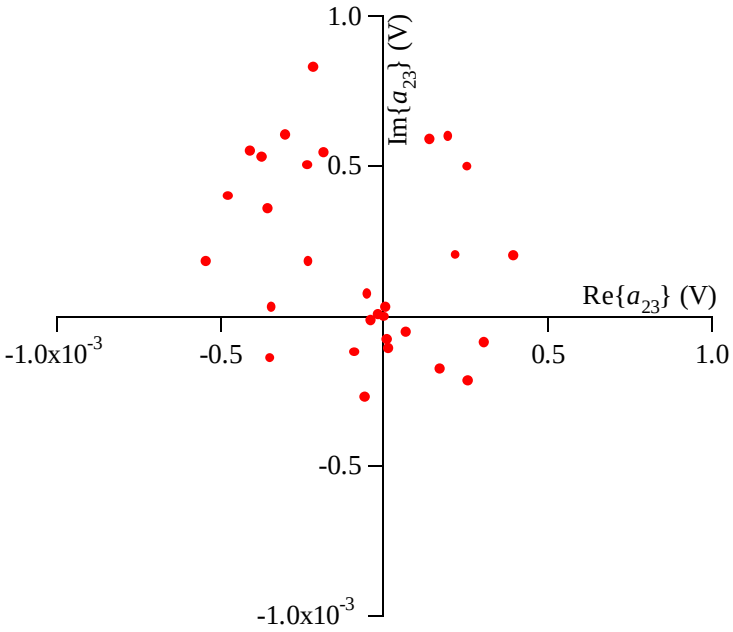

Figure 10. Thirty measurements of a_{23} in the complex plane with the excitation from source 1 held constant and the output from source 2 set to random phases with constant amplitude.

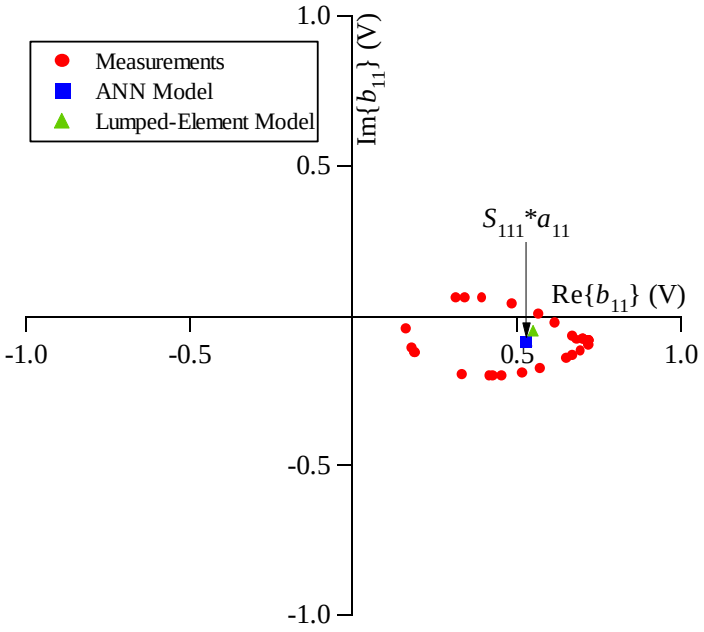

Figure 11. Thirty measurements of b_{11} in the complex plane with the excitation from source 1 held constant and the output from source 2 set to random phases with constant amplitude. Values of S_{111}•a_{11} determined from the measurement-based ANN model and the harmonic balance simulation using an equivalent-circuit model are also shown.

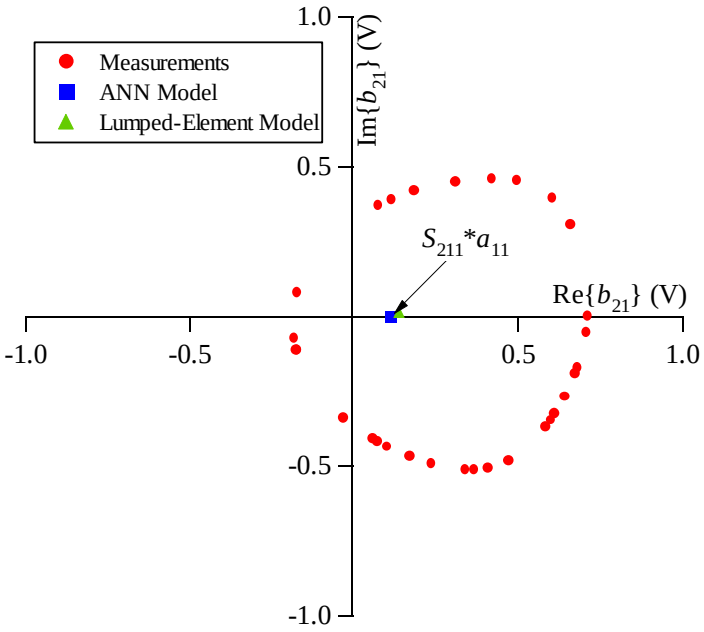

Figure 12. Thirty measurements of b_{21} in the complex plane with the excitation from source 1 held constant and the output from source 2 set to random phases with constant amplitude. Values of S_{211}•a_{11} determined from the measurement-based ANN model and the harmonic balance simulation using an equivalent-circuit model are also shown.

V. COMPARISON

We compared our results to a compact, equivalent-circuit model provided by the manufacturer and simulated in commercial harmonic-balance software to get an independent check on our methodology. A previous publication [9] showed that harmonic-balance simulations of this compact, equivalent-circuit diode model compare to the measured values of *b*'s to within 3%. Our comparison was accomplished by providing the simulator with the identical biasing conditions on the diode and a stimulus of the same magnitude used in the measurements for a_{11} and setting all other *a*'s to zero. Providing the simulated circuit with a_{11} of the same magnitude as the measurement should give the same values of b_{11} and b_{21} as the interpolated values of b_{11} ($=S_{111}\bullet a_{11}$) and b_{21} ($=S_{211}\bullet a_{11}$) determined by the ANN models when a_{12}, a_{13}, a_{21}, a_{22}, and a_{23} are equal to zero. Figures 11 and 12 show that these simulated values b_{11} and b_{21} agree with those determined from the measurement-based ANN models. Quantitatively, the differences between the ANN and equivalent-circuit models are 2.51% for b_{11} and 3.93% for b_{21}.

VI. CONCLUDING REMARKS

We have described a method of generating nonlinear large-signal scattering parameters (S_{ijk}) as a function of bias level and excitation level over a pre-selected range of parameters using a nonlinear vector network analyzer. We used a second source and multiple measurements of a nonlinear circuit to train artificial neural networks that yield portable models that are independent of the measurement instrumentation. We checked our approach by comparing our results to a compact, equivalent-circuit model simulated in commercial harmonic-balance software, and showed that the two methods agree well.

There are many possible applications of nonlinear large-signal scattering parameters. For example, the source impedance required for conjugate match (maximum power transfer) at the excitation frequency of a nonlinear device may be obtained from S_{111} at the large-signal operating point. Similarly, S_{221} can be used to select the optimum output load impedance at the fundamental frequency in a power amplifier. Values of S_{221} could also be obtained not only for a specified input power level (a_{11}) but also for specified terminations at various harmonics (a_{2k}/b_{2k}). In addition to power-amplifier applications, S_{22k} could also be used to select the optimum load impedance for the output at the *k*th harmonic for a frequency multiplier. We are currently investigating various applications of nonlinear large-signal scattering parameters and will report on them as results are obtained.

Advantages of developing such frequency-domain models for nonlinear circuits include the ability to link model accuracy to measurements and the elimination of the transformation from time-domain to frequency-domain currently required in harmonic-balance analysis to accelerate simulation time.

ACKNOWLEDGMENTS

We thank Jim Booth of NIST for his helpful suggestions regarding the preparation of this manuscript, and Marc Vanden Bossche and Jan Verspecht of Agilent Technologies, Inc. for their helpful discussions.

REFERENCES

[1] M. Sipila, K. Lehtinen, V. Porra, "High-frequency periodic time-domain waveform measurement system," *IEEE Trans. Microwave Theory Tech.*, vol. 36, pp. 1397-1405, Oct. 1988.

[2] U. Lott, "Measurement of magnitude and phase of harmonics generated in nonlinear microwave two-ports," *IEEE Trans. Microwave Theory Tech.*, vol. 37, pp. 1506-1511, Oct. 1989.

[3] G. Kompa and F. Van Raay, "Error-corrected large-signal waveform measurement system combining network analyzer and sampling oscilloscope capabilities," *IEEE Trans. Microwave Theory Tech.*, vol. 38, pp. 358-365, Apr. 1990.

[4] J. Verspecht, P. Debie, A. Barel, and L. Martens, "Accurate on wafer measurement of phase and amplitude of the spectral components of incident and scattered voltage waves at the signal ports of a nonlinear microwave device," *1995 IEEE MTT-S Int. Microwave Symp. Dig.*, vol. 3, pp. 1029-1032, May 1995.

[5] J. Verspecht, "Calibration of a measurement system for high-frequency nonlinear devices," Doctoral Dissertation, Vrije Universiteit Brussel, Brussels, Belgium, 1995.

[6] J. Verspecht and P. Van Esch, "Accurately characterizing hard nonlinear behavior of microwave components with the nonlinear network measurement system: introducing nonlinear scattering functions," *Proc. 5th Annual Workshop on INMMC*, pp.17-26, Duisburg, Germany, Oct. 1998.

[7] Q. J. Zhang and K. C. Gupta, *Neural Networks for RF and Microwave Design*, Artech House, 2000.

[8] NeuroModeler, ver. 1.2, Q. J. Zhang and his neural network research team, Department of Electronics, Carleton University, Ottawa, Canada, 1999.

[9] K. A. Remley, D. C. DeGroot, J. A. Jargon, and K. C. Gupta, "A method to compare vector nonlinear network analyzers," *2001 IEEE MTT-S Int. Microwave Symp. Dig.*, vol. 3, pp. 1667-1670, May 2001.